Quaternary Science Reviews 25 (2006) 3294–3311

Glacial rapid variability in deep-water temperature and $\delta^{18}O$ from the Western Mediterranean Sea

Isabel Cacho[a,b,*], Nick Shackleton[a], Harry Elderfield[a], Francisco J. Sierro[c], Joan O. Grimalt[d]

[a] *The Godwin Laboratory for Palaeoclimate Research, Department of Earth Sciences, University of Cambridge, Downing Street, Cambridge CB2 3EQ, UK*
[b] *GRC Marine Geosciences, Department of Stratigraphy, Palaeontology and Marine Geosciences, Faculty of Geology, University of Barcelona, C/Martí i Franqués, s/n, E-08028 Barcelona, Spain*
[c] *Department of Geology, University of Salamanca, Plaza de la Merced s/n. 37008, Salamanca, Spain*
[d] *Department of Environmental Chemistry, Institute of Chemical and Environmental Research (CSIC), Jordi Girona, 18, 08034 Barcelona, Spain*

Received 22 December 2005; accepted 19 October 2006

Abstract

Deep-water temperatures (DWTs) from the Western Mediterranean Sea are reconstructed for the last 50 ka based on the analysis of Mg/Ca ratios in benthic foraminifera from core MD95-2043 collected in the Alboran Sea. The exceptionally high sedimentation rates of this core and the robust chronology available allow discussion of the results in the context of the Dansgaard–Oeschger (D–O) rapid climatic variability. The applicability of Mg/Ca thermometry in the Western Mediterranean Deep-Water mass (WMDW) is first tested by the analysis of different benthic species in a collection of Mediterranean core tops. The results indicate the need of a readjustment of the existing *Cibicidoides* spp. calibrations in order to reconstruct present Western Mediterranean DWT values (12.7 °C). Different physiological effects in the Mg uptake between the *C. pachydermus* living in different regions could account for this offset in the Mediterranean samples. Consequently, the obtained DWT record still has many uncertainties in absolute terms but trends provide valuable information on past changes in WMDW conditions. The DWT record shows significant oscillations in relation to the D–O cycles, colder values occurred during the time of D–O stadials and warmer ones during D–O interstadials. Surprisingly, the coldest DWTs occurred during the time of Heinrich Event 4 (HE4) and not during the Last Glacial Maximum (LGM) when DWTs were mostly warm. These and other particular features of the DWT reconstruction mimic changes in the vegetation from the Eastern Mediterranean indicating the control of the Mediterranean climate on the DWT record. Paired analyses of Mg/Ca and δ^{18}Occ (calcite δ^{18}O) provide the opportunity to reconstruct deep-water δ^{18}O (δ^{18}Odw) and past salinities and hence changes in past WMDW density. Due to the large error associated with these calculations, they can only be discussed in terms of relative changes between different intervals. The results suggest the dominance of a heavier water end member during glacial times and a lighter one during the early Holocene in relation to the δ^{18}Odw conditions present today. Densest WMDW were formed during most of Marine Isotopic Stage (MIS) 2 and during the D–O Stadials not associated with HEs, while lightest WMDW dominated during D–O Interstadials. The δ^{18}Odw record shows a D–O variability pattern likely controlled by changes in the composition and intensity of the local run-off and also to changes in the δ^{18}Ow signal of the Atlantic inflow. Changes in the residence time of the Mediterranean waters, governed by the global sea level, are also considered to exert an important role governing Mediterranean δ^{18}Ow and salinity, particularly during MIS 2. Overall, our results are consistent with the formation of dense WMDW during D–O stadials and even denser during most of MIS 2.

1. Introduction

The semi-arid climatic regime of the Mediterranean region leads to a negative precipitation–evaporation balance and hence this semi-enclosed basin acts as a concentration basin (Béthoux, 1979; Pinardi and Masetti, 2000). Relatively dense water masses are formed and sink to a great depth in very specific regions such as the Gulf of

*Corresponding author. GRC Marine Geosciences, Department of Stratigraphy, Palaeontology and Marine Geosciences, Faculty of Geology, University of Barcelona, C/Martí i Franqués, s/n, E-08028 Barcelona, Spain. Tel.: +34 934034641; fax: +34 934021340.

E-mail address: icacho@ub.edu (I. Cacho).

0277-3791/$ - see front matter © 2006 Elsevier Ltd. All rights reserved.
doi:10.1016/j.quascirev.2006.10.004

Lions where Western Mediterranean Deep Water (WMDW) is formed (Lacombe et al., 1985). The Eastern Mediterranean Sea has two main convection cells, one in the Levantine Basin where Levantine Intermediate Water (LIW) forms and the other in the Adriatic Sea (sometimes switching to the Aegean Sea) where the Eastern Mediterranean Deep-Water mass is formed (EMDW). All these convection cells are interconnected as LIW is one of the main contributors to the EMDW and WMDW (Pinardi and Masetti, 2000).

Deep-water overturning is controlled by regional evaporation but also by the local wind systems over these areas. The flow of relatively dry and cold north winds intensifies water evaporation and promotes cooling but also adds kinetic momentum, which allows water to sink (Lacombe et al., 1985; Millot, 1990). As a consequence, changes in the intensity of these overturning Mediterranean cells can provide a good diagnosis of the dominant climatic conditions in the region. These Mediterranean water masses are also relevant to the North Atlantic Ocean as they export the Mediterranean Outflow Water (MOW) that is fed by a mixture of modified LIW and WMDW. The MOW forms a salt injection into the intermediate Atlantic Ocean and can have a potential impact on deep-water production in the Nordic Seas (Reid, 1979). It has been hypothesized that changes in the MOW intensity could have been more relevant in the North Atlantic deep overturning in the past (Bigg et al., 2003). In particular, model results suggest that brief but large increases in MOW strength could have led the North Atlantic to return to strong overturning mode (Bigg and Wadley, 2001). In this respect, changes in the MOW intensity in relation to glacial–interglacial climatic variability and sapropel production have been documented previously (Zahn et al., 1987; Rohling, 1994). More recently, high resolution records from the Western Mediterranean Sea have provided solid evidence for centennial–millennial changes in the ventilation rate of WMDW following D–O climatic variability (Cacho et al., 2000; Sierro et al., 2005). Drift deposits from the Gulf of Cadiz support MOW strengthening during times of enhanced WMDW overturning (Voelker et al., 2006).

The application of Mg/Ca palaeothermometry on benthic foraminifera brings a unique opportunity to reconstruct, in absolute terms, changes in deep-water properties. Use of Mg/Ca palaeothermometry is increasing rapidly in palaeoceanographic reconstructions particularly in planktonic foraminifera (Barker et al., 2005 and references therein). However, benthic reconstructions are still very scarce and the calibrations available are very limited in number and species and need further improvement (Rosenthal et al., 1997; Lear et al., 2002; Martin et al., 2002; Marchitto and deMenocal, 2003; Marchitto et al., in press). This study presents the first reconstruction of deep-water temperature (DWT) and $\delta^{18}O$ (δ^{18}Odw) from the Western Mediterranean Sea. This reconstruction is based on paired measurements of Mg/Ca and stable isotopes in *C. pachydermus* from the IMAGES core MD95-2043 recovered in the Alboran Sea (Western Mediterranean Sea). Previous studies have documented the high quality of this core for palaeoceanographic and palaeoclimatic studies covering the last 50 ka (Cacho et al., 1999; Pérez-Folgado et al., 2003; Moreno et al., 2005 and references therein). The benthic isotopes from this core were reported in a previous study but at lower resolution than presented here and concentrating only on MIS 3 (Cacho et al., 2000). This previous study proposed a model of D–O variability for WMDW formation consisting of stadial stimulation in deep ventilation produced by a reinforcement of the north westerlies flowing over the WMDW source area (Gulf of Lions). A subsequent study performed on a higher resolution record from the North of Menorca (MD99-2343) confirms this model of variability but suggests a more complex pattern for those stadials in which Heinrich Events (S-HE) occurred (Sierro et al., 2005).

The present study provides the first reconstruction of the WMDW temperature changes associated with D–O variability during the MIS 3 and the LGM and, at lower resolution, during deglaciation and Holocene periods. Since *C. pachydermus* disappears during the deglaciation, the record is supplemented by a few analyses performed on alternative benthic species such as *Gyroidina altiformis* and *Gyroidina neosoldanis*. In order to test the suitability of the current benthic calibrations in the context of this Mediterranean region, we have also analysed different benthic species in a set of core top samples taken from a wide area of the Western Mediterranean Sea. These core top results are compared to water measurements to give an insight on the feasibility of our geochemical approach for reconstructing reliable temperature, δ^{18}Odw and salinity conditions of WMDW.

2. Material and methods

Reconstructions of past Mediterranean conditions are based on the analysis of core MD95-2043 (36°8.6′N; 2°37.3′W; 1841 m water depth) recovered from the Alboran Sea (Western Mediterranean Sea) during the 1995 IMAGES-I Calypso coring campaign onboard R/V *Marion Dufresne* (Fig. 1). The chronological model for this core was previously presented and discussed (Cacho et al., 1999). Briefly, it is based on 17 calibrated AMS ^{14}C dates for the last 20 ka and on visual correlation between the alkenone sea surface temperature record of this core and the ice $\delta^{18}O$ from GISP2 for the interval between 20 and 50 ka BP (Cacho et al., 1999). Present or near-present conditions of the WMDW have been reconstructed from measurements of core top samples from a set of multi-cores recovered from a wide area of the Western Mediterranean Sea (Table 1 and Fig. 1). These core top samples integrate a water depth range of 630–2850 m; the current water mass filling those depths is the WMDW, which is also the water mass over the position of Core MD95-2043.

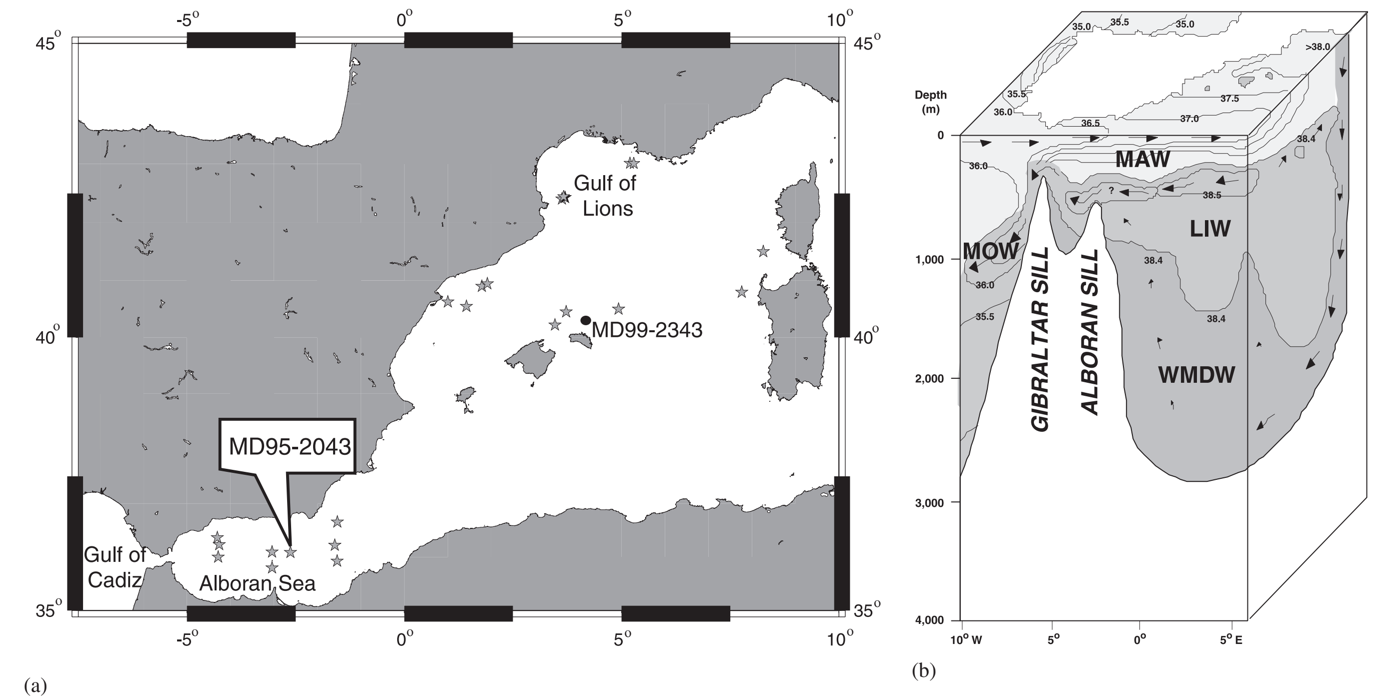

Fig. 1. (a) Location of the studied core (MD95-2043), the stars indicate the position of the core top stations (Table 1). (b) 3D diagram of the Western Mediterranean Sea showing the situation of the different water masses and the location of the deep convection cell of the WMDW (Gulf of Lions).

Table 1
Geographical information on the core tops included in this study

Core top	Location	Water depth (m)	Latitude	Longitude
CTA1	Alboran Sea (W)	654	36°22.05′N	4°18.14′W
CTA2	Alboran Sea (W)	962	36°14.31′N	4°15.52′W
CTA3	Alboran Sea (W)	1300	36°00.31′N	4°17.04′W
CTA4	Alboran Sea (E)	1750	36°06.09′N	3°02.41′W
CTA5	Alboran Sea (E)	1824	36°05.54′N	2°37.28′W
CTA6	Alboran Sea (E)	1993	35°55.74′N	1°32.59′W
CTA7	Alboran Sea (E)	2016	36°39.63′N	1°32.35′W
CTG1	Gulf of Lions (Eix Marseille canyon)	1180	43°00.65′N	5°11.62′E
CTG2	Gulf of Lions (Interfluve Marseille canyon)	630	43°00.43′N	5°16.83′E
CTG3	Gulf of Lions (Eix Lacaze canyon)	1175	42°24.24′N	3°37.63′E
CTG4	Gulf of Lions (Interfluve Lacaze canyon)	780	42°25.73′N	3°41.96′E
CTG5	Gulf of Lions (Interfluve Lacaze canyon)	732	42°26.60′N	3°39.87′E
CTC1	Cat-Bal Sea (Interfluve Foix canyon)	1040	40°54.02′N	1°47.05′E
CTC2	Cat-Bal Sea (Eix Foix canyon)	1310	40°56.65′N	1°54.68′E
CTC3	Cat-Bal Sea (Ebro slope)	625	40°32.93′N	1°25.85′E
CTC4	Cat-Bal Sea (Balearic Platform)	601	40°13.13′N	3°28.11′E
CTC5	Cat-Bal Sea (Balears)	2065	40°27.17′N	3°43.38′E
CTB1	Balearic Abyssal Plane	2336	41°30.16′N	8°15.64′E
CTB2	Balearic Abyssal Plane	2850	40°30.00′N	4°55.76′E
CTB3	Balearic Abyssal Plane	2696	40°47.82′N	7°45.85′E

2.1. Trace element measurements

The analysed foraminifera were picked from the fraction over 250 μm, each sample consisting of 5–10 specimens in the case of *C. pachydermus,* 8–25 in the case of *Gyroidina* spp. and 10–15 specimens for *Uvigerina mediterranea*. Foraminifera were carefully crushed between glass slides under the microscope in order to check the aperture of the chambers but preventing their over-crushing, which would promote sample loss during the cleaning procedure. After crushing, the sample was homogenized and split in two sub-samples, two thirds of the sample were transferred to acid leached vials for the trace element measurements and the rest saved for isotopic measurements.

The cleaning procedure undertaken has been elaborated from that originally published by Boyle (1981) and Boyle and Keigwin (1985) with some minor changes, which mainly consist of the elimination of the so-called reductive step (Barker et al., 2003). The procedure consists of three phases: clay removal, oxidation and weak acid leaching. The first phase consists of three water cleanings by ultrasonic stirring and posterior stimulation of clay re-suspension and two additional methanol washings. For the second step 250 µl of hydrogen peroxide were dissolved in 15 ml of 0.1 M NaOH and 250 µl of this solution were added to each sample and kept in a hot bath for 15 min. The third step was performed in 250 ml of 0.001 M ultra-pure HNO_3 stirring the sample in an ultrasonic bath for 10 s. Instrumental analysis was performed by ICP-AES after addition of 400 µl of ultra-pure 0.075% HNO_3 to each sample and sonication. Sample dissolution and instrumental measurements were performed in the same day.

The analyses were performed in a Varian Vista AX simultaneous inductively coupled plasma atomic-emission spectrometer at the Department of Earth Sciences (University of Cambridge) following the conditions published by de Villiers et al. (2002). At the time of analysis of most *C. pachydermus* samples from core MD95-2043 only Mg, Ca and Sr were measured. Subsequently, at the time of analysis of the core tops, *Gyroidina* spp. samples from MD95-2043 and a few replicates of *C. pachydermus* samples from MD95-2043 additional elements were monitored, in particular Mn and Fe, for the identification of potential contamination problems from clays or Mn-rich carbonates (Barker et al., 2003; Pena et al., 2005).

2.2. Stable isotopes measurements

Oxygen and carbon isotope ratios (δ^{18}Occ and δ^{13}C) were analysed in aliquots representing one-third of the samples crushed for trace element measurements (see Section 2.1). This strategy provides a homogeneous sample mixture for both trace elements and isotopic measurements and minimized the errors in the reconstruction of the δ^{18}Odw values.

Prior to the analyses, the samples were cleaned with hydrogen peroxide. Isotope analyses were performed in the Godwin Laboratory (Cambridge University) on a Micromass Multicarb Sample Preparation System attached to a PRISM mass spectrometer. Measurements were determined in relation to the Vienna Peedee Belemnite (VPDB) standard, with an analytical precision that is better than 0.08‰ for the δ^{18}O and 0.06‰ for the of δ^{13}C measurements.

2.3. Estimations of δ^{18}Odw and deep-water salinity

C. pachydermus δ^{18}Occ values were adjusted to those of *Uvigerina* by adding 0.5‰ to the measured δ^{18}Occ (Shackleton, 1974). δ^{18}Odw was estimated after extracting the temperature effect according to the DWT estimates based on the Mg/Ca ratios measured in the same benthic foraminifera. Temperature correction was performed according to the O'Neil's equation (O'Neil et al., 1969; Shackleton, 1974). Results were transferred to SMOW by adding a standard correction of 0.27‰ to the δ^{18}Occ. The resulting δ^{18}Odw estimates integrate the combined signal from global glacioeustatic changes and the local δ^{18}O variability in water masses. The global glacioeustatic effect can be corrected (δ^{18}Odw-ice) using the sea level reconstructions from Lambeck and Chappell (2001) for the 0–22 ka BP interval and from Siddall et al. (2003) for the 22–50 ka BP interval. In palaeoceanographic reconstructions the residual δ^{18}Odw-ice estimates are frequently assumed to be directly linked to past changes in salinity. But a critical issue is the selection of accurate salinity:-δ^{18}Ow relationships for such estimation. Salinity:δ^{18}Ow relationships are highly regional and often seasonally dependent. In the present study a salinity:δ^{18}Ow relationship has been estimated using the data from Mediterranean source water masses (Pierre, 1999) (accessible on: http://data.giss.nasa.gov/o18data/) but excluding the data of waters from the Atlantic inflow. Significant differences in the slope of the salinity: δ^{18}Ow relationships were obtained between the water masses from Atlantic and Mediterranean sources. The following equation was obtained from the integration of data from both Western and Eastern Mediterranean water masses below 150 m:

$$\text{Salinity} = (\delta^{18}\text{O}_\text{w} + 17.378)/0.4896 \quad (r = 0.7; n = 215).$$

3. Results and discussion

3.1. Potential interferences in the Mg/Ca record

Mg/Ca ratios in foraminifera tests can be affected by post-depositional processes which induce inaccuracies in the temperature reconstructions. Carbonate dissolution and the presence of silicates or diagenetic minerals are the main potential sources for these Mg/Ca biases. Analyses in planktonic foraminifera have shown that partial dissolution of the carbonate tests results in a lowering of the Mg/Ca ratio since the Mg-enriched carbonate dissolves preferentially (Brown and Ederfield, 1996). Benthic foraminifers are expected to be less sensitive to dissolution processes but some effect could still be expected. The Fragmentation Index (FI), measured as the percentage of fragmented foraminifera tests in the samples, can be used as a proxy for dissolution (Fig. 2a and b) (Hodell et al., 2001). Mg/Ca variability does not show co-variation with the FI, with the exception of the warming at the base of the record, which correlates with an increase in the FI. Higher dissolution would have induced a Mg/Ca lowering and thus colder DWT. In consequence dissolution could have accounted for a small bias in the quantitative reconstruction but trends in the record were not shaped by dissolution processes.

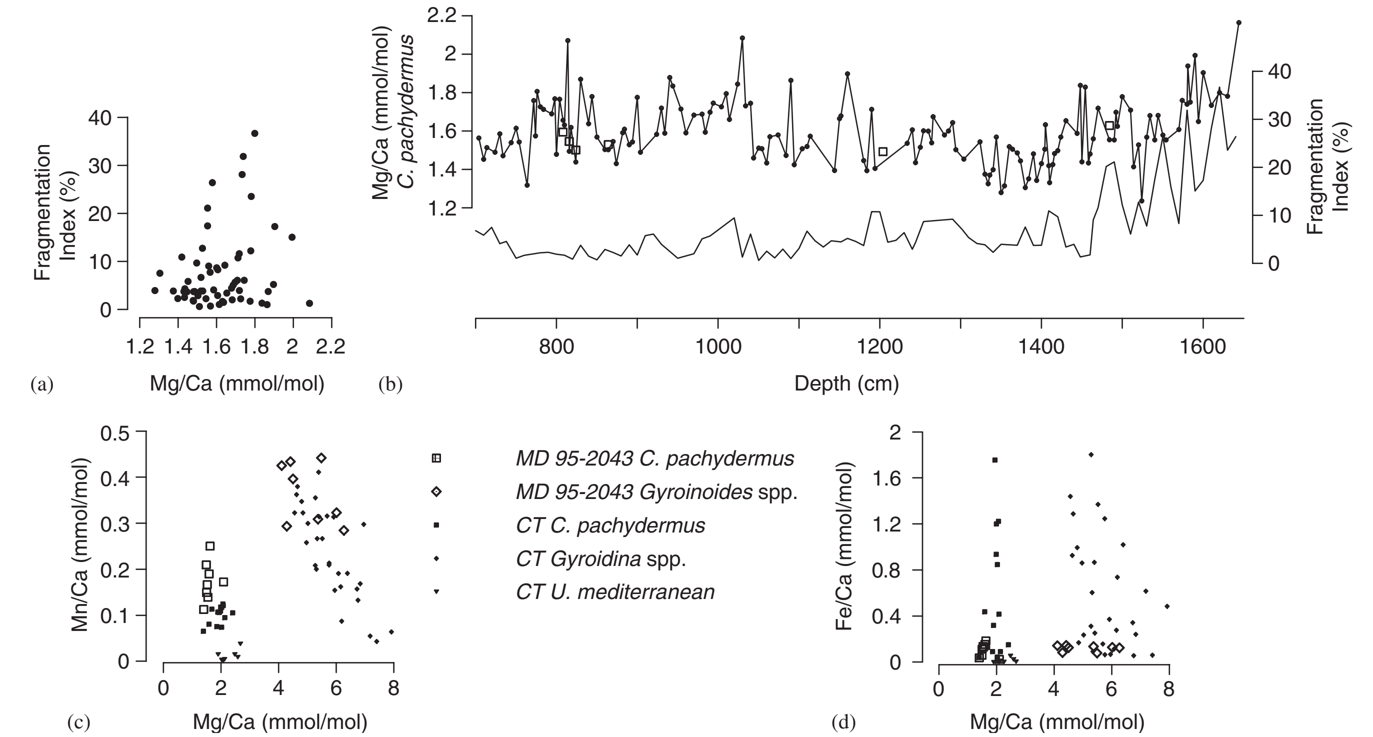

Fig. 2. (a) Mg/Ca ratios measured in *C. pachydermus* plotted versus the Fragmentation Index (FI), both measured in core MD95-2043; (b) Depth profile from Mg/Ca and FI from core MD95-2043. (c) Mn/Ca and (d) Fe/Ca ratios plotted versus Mg/Ca for different species of benthic foraminifera in core MD95-2043 and core top samples from multicores.

Contamination of Mg/Ca ratios from materials other than foraminifera carbonates can be monitored by the parallel analysis of different symptomatic elements. In this respect, the presence of Fe and Al may be indicative of clay minerals (Barker et al., 2003) or volcanic debris (Lea et al., 2005). On the other hand, Mn may indicate contributions from Mn-rich carbonate phases (Pena et al., 2005). However, high values in the diagnosis ratios of these elements may not necessarily involve Mg contamination. At the time when the MD95-2043 data set for *C. pachydermus* was generated none of the diagnostic ratios involving these elements were determined. Later, when core top samples were processed Fe/Ca and Mn/Ca ratios were measured in parallel with Mg/Ca (Fig. 2c and d). A few *C. pachydermus* samples from MD95-2043 were also replicated together with some new *Gyroidina* spp. samples, and all these analyses included Fe/Ca and Mn/Ca measurements (Fig. 2c and d).

The Mn/Ca ratios obtained are very variable depending on the species analysed (Fig. 2c). In this way, the lowest Mn/Ca ratios are for *U. mediterranea* (about 0.01 mmol/mol), Mn/Ca exhibited maximal values in the MD95-2043 *Gyroinoidines* spp. samples (average of 0.36 mmol/mol) and core top *Gyroidina* spp. samples showed a very large variability (0.04–0.38 mmol/mol) but with a dominance of relatively high values (Fig. 2c). *C. pachydermus* showed higher Mn/Ca ratios for the samples from MD95-2043 (0.17 mmol/mol). However, these Mn/Ca ratios are still low in comparison to those measured in samples contaminated with Mn-rich carbonate (0.5–7 mmol/mol) (Pena et al., 2005). Furthermore, the absence of any linear relationship between Mn/Ca and Mg/Ca ratios supports the lack of Mg contamination by Mn-carrier phases such as Mn-oxides or Mn-rich carbonates (Fig. 2c).

Fe/Ca ratios are in general very high (Fig. 2d). The highest values are found for both *C. pachydermus* and *Gyroidina* spp. samples from the core tops but with a large spread (0.04–1.75 and 0.05–2.78 mmol/mol, respectively) while downcore ratios for both species are much lower (about 0.10 and 0.12 for *C. pachydermus* and *Gyroidina* spp., respectively). These values are in the range of or even higher than those measured in samples contaminated with volcanic detritus (0.05–0.6 mmol/mol) (Lea et al., 2005) but below the 0.1 mol/mol threshold proposed by Barker et al. (2003) as the rejection criteria to discriminate between clean and silicate contaminated samples. Fe/Mn ratios for the core top samples range between 2 and 5 mol/mol, which is very high in comparison to those attributed to ferromanganese overgrowths (0.8 mol/mol) (Skinner and Elderfield, 2005). All this evidence points towards the presence of some silicates in the core top samples, but the lack of co-variance of these Fe/Ca ratios with Mg/Ca ratios suggests that Mg may not be a major constituent of the contaminant phase (Fig. 2d). The presence of silicates appears to be less critical in samples from core MD95-2043, where good reproducibility obtained in a few replicates suggests that random noise derived from the presence of silicates is not a major problem (square points in Fig. 2b).

3.2. Reconstruction of present deep-water properties

3.2.1. DWT estimations

Near-present WMDW conditions have been estimated from the analysis of different benthic species (*C. pachydermus, Gyroidina* spp. and *U. mediterranea*) from a series of W Mediterranean core tops. The collection of core tops covers a wide area of the Western Mediterranean Sea and a range of 600–2300 m water depth, which is the main domain of the WMDW. Current water temperatures at these depths are rather constant 12.7±0.5 °C (Pierre, 1999; MEDATLAS, 2002), and ideally, all the core top Mg/Ca measurements should reflect this average temperature. *C. pachydermus* is not a dominant species in the present sediments and it has only been found in 12 of the 19 locations studied (Table 2). However, it was not always sufficiently abundant to perform both isotopic and Mg/Ca measurements.

Analysis of δ^{18}O allowed cross-checking against reworked material from glacial ages. Those samples exhibiting high (glacial) isotope values were excluded in the estimations and averages (italic numbers in Table 2). Mg/Ca ratios measured in *C. pachydermus* from the core top series of the present study range between 1.89 and 2.13 mmol/mol with the exception of the only sample available in the context of the Alboran Sea (CTA1) which provided significantly lower values 1.69 mmol/mol. CTA1 was recovered from a relatively shallow part of the Alboran Sea (600 m) below the Malaga upwelling system. Further measurements including more systematic samplings of the area are needed in order to interpret this result. We have considered an average value of 1.96 mmol/mol to represent Mg/Ca values from *C. pachydermus* in the domain of current WMDW (Table 3). DWT can be estimated using the Mg/Ca-temperature calibration defined for common *Cibicidoides* species in a temperature range of 0.8–18 °C (Lear et al., 2002)

$$\mathrm{Mg/Ca} = 0.867 \pm 0.049 \exp(0.109 \pm 0.007 \times \mathrm{DWT}).$$

The temperature sensitivity of this calibration is very similar to others previously published for *Cibicidoides* spp., but also to that estimated for different species of planktonic foraminifera (Rosenthal et al., 1997; Lear et al., 2002; Anand et al., 2003). Considering the associated errors in the exponential and pre-exponential terms of the calibration, DWT estimates should be better than ±1 °C (Lear et al., 2002). The estimated DWT for our core tops using this calibration is 7.5 °C, about 5 °C colder than the average measured values (12.7 °C). This temperature estimate is far colder than any water mass in the

Table 2
Data on isotopes and trace elements on the core top samples

Sample code	*Cibicidoides pachydermus*				*Uvigerina mediterranea*				*Gyroinoides* spp. (soldani + altiformis)			
	δ^{18}Occ (‰ VPDB)	δ^{13}C (‰ VPDB)	Mg/Ca (mmol/mol)	Sr/Ca (mmol/mol)	δ^{18}Occ (‰ VPDB)	δ^{13}C (‰ VPDB)	Mg/Ca (mmol/mol)	Sr/Ca (mmol/mol)	δ^{18}Occ (‰ VPDB)	δ^{13}C (‰ VPDB)	Mg/Ca (mmol/mol)	Sr/Ca (mmol/mol)
CTA1	1.58	0.59	1.69	1.33	2.07	0.21	1.90	1.22	2.04	−1.02	4.63	1.28
CTA2							*2.67*	*1.26*	2.03	−1.11	4.66	1.26
CTA3									1.76	−1.23	6.39	1.30
CTA4									1.79	−1.55	4.97	1.30
CTA5									1.83	−1.33	4.56	1.26
CTA6									1.81	−1.28	5.75	1.28
CTA7									1.74	−1.26	6.73	1.30
CTG1	1.65	1.05	2.02	1.31	2.27	−0.01	2.08	1.25	1.86	−1.27	5.31	1.37
CTG2			*2.40*	*1.38*					1.78	−1.02	5.34	1.38
CTG2	1.66	1.11	2.13	1.37					1.91	−1.01	7.92	1.36
CTG3			*1.59*	*1.32*			*2.25*	*1.22*	1.79	−1.21	6.96	1.37
CTG4			*2.03*	*1.37*	2.24	0.56	2.48	1.20	1.65	−0.99	5.69	1.38
CTG5	*2.15*	*1.24*	*2.08*	*1.37*	2.05	0.15	2.02	1.24	1.74	−1.35	5.02	1.36
CTC1	1.58	0.60	1.94	1.35					1.76	−1.43	5.28	1.32
CTC2	1.73	0.58	1.99	1.32					1.86	−1.32	5.91	1.34
CTC3	1.62	0.45	2.07	1.36	2.18	−0.09	2.59	1.22	1.95	−1.28	5.39	1.31
CTC4	*3.88*	*1.66*	*1.86*	*1.47*	2.10	0.48	2.12	1.25	*2.26*	*−0.64*	*6.83*	*1.42*
CTC5									1.88	−0.94	6.76	1.30
CTB1	1.59	1.10							1.84	−0.97	7.18	1.35
CTB2									1.83	−1.22	6.16	1.33
CTB3	1.62	0.83	1.89	1.33					1.79	−1.42	4.85	1.40
CTB3	1.65	0.89	1.98	1.32					1.76	−1.30	5.52	1.24

Numbers in italic indicate the values not included in average estimations (see text).

Table 3
Deep water temperature (DWT), δ^{18}Odw and salinity estimations for the analysed core tops compared to current water data

Sample code	*Cibicidoides pachydermus* δ^{18}Occ (‰ VPDB)	Mg/Ca (mmol/mol)	DWT (°C)	δ^{18}Odw (‰ VSMOW)	Salinity (PSU)	*Uvigerina mediterranea* δ^{18}Occ (‰ VPDB)	Mg/Ca (mmol/mol)	DWT (°C)	δ^{18}Odw (‰ VSMOW)	Salinity (PSU)	*Gyroinoides* spp. (soldani + altiformis) δ^{18}Occ (‰ VPDB)	Mg/Ca (mmol/mol)	DWT (°C)	δ^{18}Odw (‰ VSMOW)	Salinity (PSU)
CTA1	1.58	1.69	11.3	1.04	37.62	2.07	1.90	11.8	1.14	37.81	2.04	4.63	10.9	0.88	37.29
CTA2							*2.67*				2.03	4.66	10.9	0.89	37.32
CTA3											1.76	6.39	14.4	1.44	38.44
CTA4											1.79	4.97	11.6	0.82	37.17
CTA5											1.83	4.56	10.7	0.63	36.79
CTA6											1.81	5.75	13.2	1.22	37.99
CTA7											1.74	6.73	14.9	1.55	38.66
CTG1	1.65	2.02	13.0	1.51	38.58	2.27	2.08	13.3	1.71	38.99	1.86	5.31	12.4	1.07	37.68
CTG2		*2.40*									1.78	5.34	12.4	1.01	37.55
CTG2	1.66	2.13	13.5	1.63	38.83						1.91	7.92	16.7	2.14	39.86
CTG3		*1.59*					2.25				1.79	6.96	15.3	1.69	38.94
CTG4		*2.03*				2.24	2.48	16.2	2.35	40.29	1.65	5.69	13.1	1.03	37.61
CTG5	*2.15*	*2.08*				2.05	2.02	12.9	1.38	38.31	1.74	5.02	11.7	0.80	37.13
CTC1	1.58	1.94	12.6	1.36	38.27						1.76	5.28	12.3	0.95	37.44
CTC2	1.73	1.99	12.9	1.56	38.68						1.86	5.91	13.5	1.35	38.25
CTC3	1.62	2.07	13.2	1.53	38.61	2.18	2.59	16.9	2.44	40.48	1.95	5.39	12.5	1.19	37.93
CTC4	*3.88*	*1.86*				2.10	2.12	13.6	1.61	38.78	*2.26*	*6.83*			
CTC5											1.88	6.76	15.0	1.70	38.98
CTB1	1.59										1.84	7.18	15.6	1.82	39.20
CTB2											1.83	6.16	14.0	1.42	38.39
CTB3	1.62	1.89	12.4	1.33	38.22						1.79	4.85	11.4	0.75	37.03
CTB3	1.65	1.98	12.8	1.47	38.49						1.76	5.52	12.8	1.07	37.68
Average	*1.63*	*1.96*	*12.7*	*1.43*	*38.41*	*2.15*	*2.20*	*14.1*	*1.77*	*39.11*	*1.75*	*5.50*	*12.51*	*1.21*	*37.97*
STDDESV	*0.05*	*0.13*	*0.65*	*0.19*	*0.38*	*0.09*	*0.27*	*1.82*	*0.47*	*0.96*	*0.09*	*0.93*	*1.71*	*0.40*	0.82

	DWT (°C)	δ^{18}Odw (‰ VSMOW)	Measured salinity (PSU)	Estimated salinity (PSU)
Water column (>600 m)	12.71	1.49	38.50	38.54

Numbers in italic indicate the values not included in average estimations (see text).

Mediterranean Sea. The exponential fit of the *C. pachydermus* calibration and to some extent, of benthic foraminifers in general, is under discussion as very few warm data support it (Lear et al., 2002; Marchitto and deMenocal, 2003; Marchitto et al., in press). New *C. pachydermus* data from the Florida Strait covering warm temperatures suggest that those early warm samples could be an artefact and support a better fit using a linear equation (Marchitto et al., in press)

$$\mathrm{Mg/Ca} = 0.12 \times \mathrm{DWT} + 1.2.$$

This linear calibration overlaps with the exponential one for temperatures below 12 °C but separates substantially for warmer temperatures. The estimated DWT for the studied core tops using this linear calibration is 6.4 °C. The Mg/Ca ratios from Mediterranean *C. pachydermus* ratios are indeed too low for the current existing calibration. Present knowledge of the factors controlling Mg-uptake by benthic foraminifera is still fragmentary but new evidence is emerging on the potential role of alternative factors to temperature, such as degree of carbonate ion saturation or salinity (Ferguson et al., 2005; Lear and Rosenthal, 2005; Rosenthal et al., 2006; Elderfield et al., in press). Several measurements performed mostly in *C. wuellestorfi* support a steeper sensitivity to temperature at the colder end of the calibration, which is interpreted to result from a carbonate ion saturation effect (Rosenthal et al, 2006; Elderfield et al., in press). Low carbonate ion saturation inhibits Mg incorporation during calcification, saturation decreases with temperature and this lowering is particularly critical below 3 °C (Elderfield et al., in press). Carbonate ion saturation from the WMDW is about 149 μmol/kg in the Alboran Sea, an estimation based on oceanographic data from MEDATLAS (2002) using the software CO2Sys (Lewis and Wallace, 1998). Therefore, the relatively high temperature and carbonate ion concentration of the WMDW at the studied location suggest a minimum sensitivity of the analysed Mg/Ca ratios to carbonate saturation. On the other hand, the salinity effect on Mg/Ca ratios needs to be explored but some data indicate a significant increase under high salinity conditions (Ferguson et al., 2005). Culture experiments in planktonic suggested a low but positive relationship between salinity and Mg/Ca, between 4% and 10% increase in Mg/Ca per unit of salinity (Nürnberg et al., 1996; Lea et al., 1999). WMDW salinity (38.5‰) is higher than most of the deep-water masses including those represented in the *C. pachydermus* calibrations (Marchitto et al., in press) and hence this effect could not account for the relatively low Mg/Ca ratios in the Mediterranean samples. Further work needs to be done to improve the constraint of the Mg/Ca calibration and for the identification of possible intra-specific or regional differences in the Mg uptake by benthic foraminifera.

For the aims of the present study we used a simplistic approach assuming that the temperature sensitivity of the Mediterranean *C. pachydermus* should be comparable for that estimated in *Cibicidoides* from other regions. We then adjust the pre-exponential constant of the equation in order to obtain realistic estimates for the current WMDW. As a result we arrive at the following equation:

$$\mathrm{Mg/Ca} = 0.61\exp(0.109 \times \mathrm{DWT}).$$

The pre-exponential term is substantially lower than that estimated for most benthic species (Lear et al., 2002) but comparable to some planktonic species (Anand et al., 2003). Our glacial Mg/Ca ratios in core MD95-2043 oscillate between 1.4 and 1.9 mmol/mol (Fig. 4) averaging 1.6 mmol/mol. DWT estimates using the global *Cibicidoides* calibration (Lear et al., 2002) would provide temperatures between 3 and 8 °C (average 5.6 °C) and thus about 7 °C colder than the present day. In contrast, those obtained with our core-top calibration provide more realistic estimates (8.5–13 °C) suggesting about 4–2 °C colder glacial WMDW. Consequently, we have applied the adjusted calibration in this reconstruction of glacial DWT as discussed in Section 3.3.1. A secondary approach has been performed, lowering the intercept value of the linear equation from Marchitto et al. (in press) in order to force it to reproduce modern WMDW temperatures from our Mg/Ca measurements. The resulting equation is

$$\mathrm{Mg/Ca} = 0.12 \times \mathrm{DWT} + 0.44.$$

This equation is also applied in our DWT reconstruction for comparison but δ^{18}Ow and salinity estimations are based on the DWT reconstructed by using the adjusted exponential calibration.

Core top measurements have been also performed with *Gyroidina* spp. and *U. mediterranea* (Table 2). The revision of the *Gyroidina* calibration is also critical for this study since this was the only species available for Mg/Ca measured in the Holocene section of core MD95-2043. No calibration based on this species has been previously reported but a few data were provided by Lear et al. (2002). The results confirm that *Gyroidina* have a Mg-enriched test in relation to other benthic species. Mg/Ca ratios measured in the Mediterranean core tops show a rather large spread of values (4.6–7.9 mmol/mol) and average 5.5 mmol/mol. This large spread could result from the mixing of two different species of *Gyroidina*. Results from other element ratios also show large variability in the *Gyroidina* measurements (Fig. 2b) indicating a potential cleaning problem for this species. We have proceeded with the revision of the calibration according to these data but the associated error should be considerable larger than that of the estimations obtained from the *C. pachydermus* ratios. As in the case of *C. pachydermus* we have changed the pre-exponential constant from the common *Cibicidoides* calibration (Lear et al., 2002) in order to force it to pass through our Mediterranean average Mg/Ca ratios which results in

$$\mathrm{Mg/Ca} = 1.71\exp(0.109 \times \mathrm{DWT}).$$

This adjusted equation also fits with the data previously published for *Gyroidina* spp. (Lear et al., 2002), providing independent support to our approach. This is still a very poorly constrained calibration for *Gyroidina* spp. and needs further improvement, but is used here as a first attempt to estimate Holocene DWT for the Holocene section of core MD95-2043.

According to previously published core top data from *Uvigerina* spp., these species seem to have less sensitivity to temperature and the estimated calibration has a considerably lower exponential constant (Lear et al., 2002)

$$\mathrm{Mg/Ca} = 0.924\exp(0.061 \times \mathrm{DWT}).$$

The *U. mediterranea* Mg/Ca ratios measured in Mediterranean core tops vary between 1.9 and 2.59 mmol/mol (average 2.2 mmol/mol) with the lowest values corresponding to sample CTA1 from the Alboran Sea, as in the case of *C. pachydermus* results. Estimated DWT according to the *Uvigerina* spp. calibration (Lear et al., 2002) is 14.1 °C, 1° warmer than the measured temperature but within the error of the published calibration.

3.2.2. Deep-water estimations of $\delta^{18}O$ and salinity

Oxygen isotopes from *C. pachydermus* range between 1.58‰ and 1.73‰ (average 1.63‰) (Table 2), which are about 0.5‰ lighter than results from *U. mediterranea* (average 2.15‰) consistent with the reported disequilibrium of *Cibicidoides* with ambient water conditions (Shackleton, 1974). δ^{18}Odw has been estimated according to the procedure described in the methodological section. *C. pachydermus* estimates provide an average value of 1.43‰ and is very close to the average of measured δ^{18}Ow (1.49‰) (Table 3).The inter-sample spread in the estimated δ^{18}Odw is comparable to that provided by water samples from the WMDW (Fig. 3a) which gives us confidence in our approach. Only one sample (CTA1) shows values that are too light, these anomalous values are also observed in

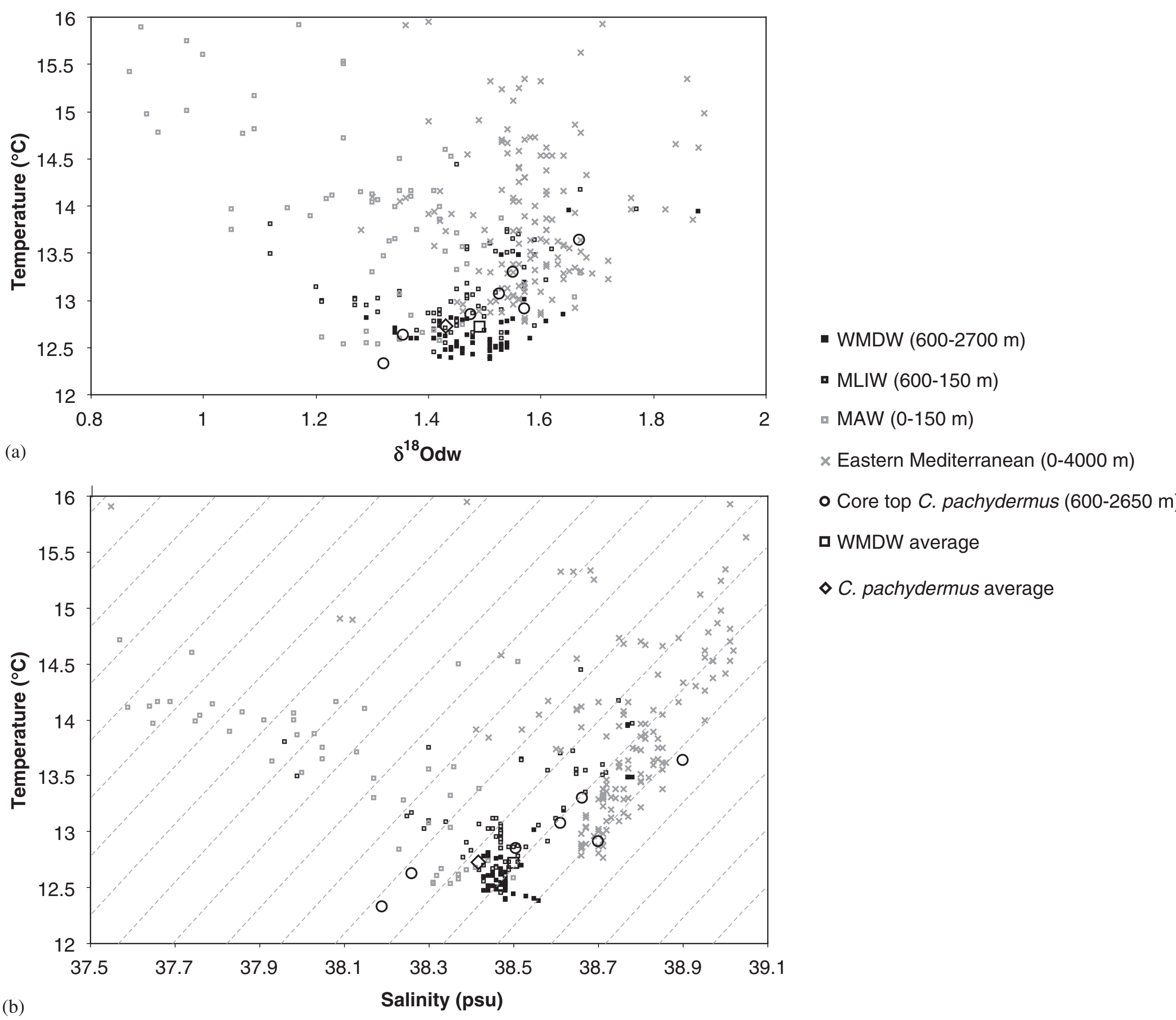

Fig. 3. Temperature-δ^{18}Ow (a) and temperature-salinity (b) diagrams for water (Pierre, 1999) and *C. pachydermus* core top samples (WMDW-Western Mediterranean Deep Water; MLIW Modified Levantine Intermediate Water; MAW Modified Atlantic Water). Grey lines in (b) are isopicnas.

U. mediterranea suggesting that they correspond to an intrinsic characteristic of the sample and not to methodological/analytical artefacts. CTA1 is the only sample representing the Alboran Sea within the *C. pachydermus* measurements but its location is very different from that of MD95-2043, since it corresponds to a shallow (600 m) location in the centre of the Malaga upwelling cell where strong vertical mixing occurs.

Local δ^{18}Odw variability is mostly dependent on changes in the ratios of evaporation to precipitation/runoff and thus co-varies with changes in local salinity. For that reason many studies have proposed the use of δ^{18}Ow to reconstruct past changes in salinity. One of the critical issues in this sort of reconstruction is the assumed relationship of seawater δ^{18}O:salinity which is highly dependent on the regional water mixing lines (Schmidt, 1999). We have reconstructed WMDW salinities, applying a specific δ^{18}Ow:salinity equation for Mediterranean water masses based on the measured data from Pierre (1999) using only those results which correspond to deep and intermediate Mediterranean water masses (see Section 2.2). The estimated equation has a relatively low correlation coefficient ($r^2 = 0.5$), as a consequence of the large spread in the measured δ^{18}Ow (Fig. 3a; Pierre, 1999). This spread suggests that δ^{18}Ow in the Mediterranean is not just controlled by evaporation rates and that other factors such as variable runoff, exert a major control on δ^{18}Ow composition. As a consequence, Mediterranean waters do not have a proportional variability between water salinity and δ^{18}Ow, which increases the uncertainty of the salinity reconstructions (Rohling, 1999). The relatively large spread in the salinity reconstructions based on our core top analyses are to some extent in agreement with this observation (Table 3 and Fig. 4b). Nevertheless, the average salinity values based on the *C. pachydermus* core top data provide a very reasonable estimate of 38.42 psu, compared to the average measured salinities, 38.5 psu, and suggests that this is still an adequate approach to reconstruct present or near-present WMDW salinity. However, its suitability to estimate past-salinity needs to be tested.

3.3. Reconstruction of past conditions

3.3.1. Past variability in Western Mediterranean deep-water properties

The new results on benthic carbon and oxygen isotopic records from core MD95-2043 confirm the previously described D–O variability, displaying low values in both oxygen and carbon isotopes during D–O interstadials and heavy values during D–O stadials (Cacho et al., 2000). These patterns are also consistent with those published recently by Sierro et al. (2005) based on *C. pachydermus* analyses from a core retrieved in a contouritic drift off the north of Menorca Island (MD99-2343). The isotopic records of both cores show a D–O type of variability in the ventilation rate of the WMDW indicating improved ventilation during the cold Stadials in contrast to the warm Interstadials (Fig. 4). These changes were linked to a strengthening of the north westerlies flowing over the northern part of the Western Mediterranean Sea, in particular over the Gulf of Lions which is the source area of this water mass (Cacho et al., 2000). Sierro et al. (2005) described a more complex pattern for the stadials coinciding with HEs (S-HEs), which included a middle interval of ventilation deterioration co-existent with anomalous light surface waters. This surface freshening presumably associated to the entrance of melt water from the North Atlantic Ocean, could have enhanced buoyancy and inhibited deep overturning during part of the S-HEs (Sierro et al., 2005). The Alboran δ^{13}C record (Fig. 4c) shows such an event for the S-HE3 and also S-HE1 but it is not clear for the others, probably as a result of the lower resolution of this record compared to the Menorca one. During the MIS 2 both oxygen and carbon isotope records show the heaviest values suggesting that ventilation was at its highest rates. Both δ^{13}C and δ^{18}Occ record a striking depletion occurring in two rapid phases at the time of the S-HE1 that marks the onset of a drastic change in the benthic conditions towards a nutrient-poor oxygen-depleted environment (Caralp, 1988) leading to the disappearance of *C. pachydermus* from the benthic assemblage. During the time of this benthic deterioration the deposition of the last organic rich layer (ORL) in the Alboran Sea also occurred (Cacho et al., 2002). *C. pachydermus* never reappeared in the Holocene section and the record has been completed with a few analyses performed on *Gyroidina* spp. Since this is an infaunal species, carbon isotopes do not provide a reliable signal of deep ventilation. δ^{18}Occ measurements suggest oxygen isotope lightening during the deglaciation (Fig. 5).

DWTs for the Western Mediterranean Sea are reconstructed based on Mg/Ca analyses performed on *C. pachydermus* samples from core MD95-2043. The Mg/Ca ratios have been expressed in temperature according to the calibration discussed in Section 3.2.1 (Fig. 4e). The record obtained shows many oscillations at high frequency (millennial–centennial time scale) which involved DWT changes of about 1–2 °C and in some cases even 4 °C; these oscillations are larger when the linear calibration is applied (Fig. 4e). This variability shows a consistent pattern of relatively cold WMDW during the D–O stadials (10–9 °C) and relatively warm temperatures during the D–O interstadials (11–13 °C), although the amplitude of these oscillations is not always proportional to the intensity of the equivalent D–O oscillations in other proxy records such as benthic isotopes or SST (Fig. 4). Interestingly, the cold DWTs reached during the S-HEs are comparable to those reached by the other D–O stadials. This is a significant difference to the SST record from the same core, which shows considerably colder temperatures for the S-HEs. Another interesting feature is that average DWTs were significantly colder during MIS 3 in comparison to MIS 2. The coldest temperatures of the record (~8 °C) occurred

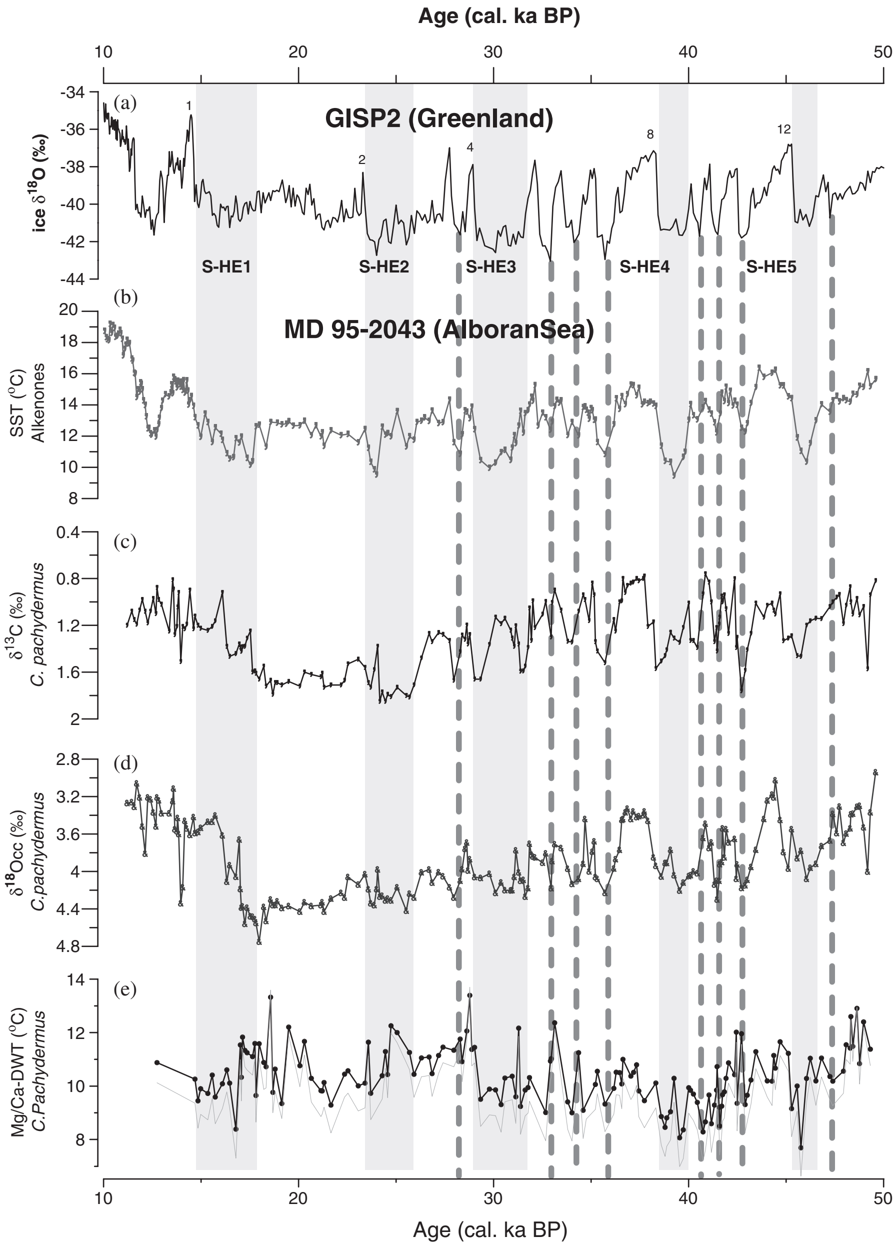

Fig. 4. Ice $\delta^{18}O$ measured in GISP2 (Meese et al., 1997) (a) compared to records measured on core MD95-2043 from the Alboran Sea (Western Mediterranean Sea): (b) Alkenone Sea Surface Temperature (Cacho et al., 1999). (c) $\delta^{13}C$ in the benthic foraminifer *C. pachydermus* with reversal *y*-axis (partially published in Cacho et al., 2000). (d) δ^{18}Occ in *C. pachydermus* (partially published in Cacho et al., 2000). (e) Deep Water Temperatures (DWT) estimations based on Mg/Ca ratios from *C. pachydermus* using the adjusted exponential calibration (black line) and the adjusted linear calibration (grey line) see Section 3.2.1. Vertical bars indicate the D–O stadials during which Heinrich Events occurred in the North Atlantic Ocean (S-HE). Chronology from Cacho et al. (1999).

slightly before and during S-HE4. DWT warmed rapidly at the end of S-HE3, and they stayed at relatively high values (over 11 °C) during most of the MIS 2 with the exception of a cold interval (20.5–23.5 cal ka BP) when DWT was about 10 °C. This cold interval is also present in the $\delta^{18}O$ from Greenland, right after the D–O interstadial 2 (about 21 ka BP). Consequently, the LGM defined as the time interval between 19 and 23 ka BP (Mix et al., 2001) was not the coldest interval in the studied DWT record. The last relatively cold interval occurred during the S-HE1 (DWT~10 °C). Holocene DWT values estimated with *Gyroidina* spp. (Fig. 5) indicate temperatures around present values (12.7 °C).

The DWT record can be used to extract the temperature component from the δ^{18}Occ. Both records share several major and minor structures although the extent of the oscillations are not always comparable (Fig. 5a). δ^{18}Odw has been estimated according to the procedure described in Section 2.3. Both δ^{18}Odw and the record after correction for the ice sheets volume (δ^{18}Ow-ice) (Lambeck and Chappell, 2001; Siddall et al., 2003) are shown in Fig. 5b. Present day WMDW δ^{18}Odw is of about 1.5‰ in good

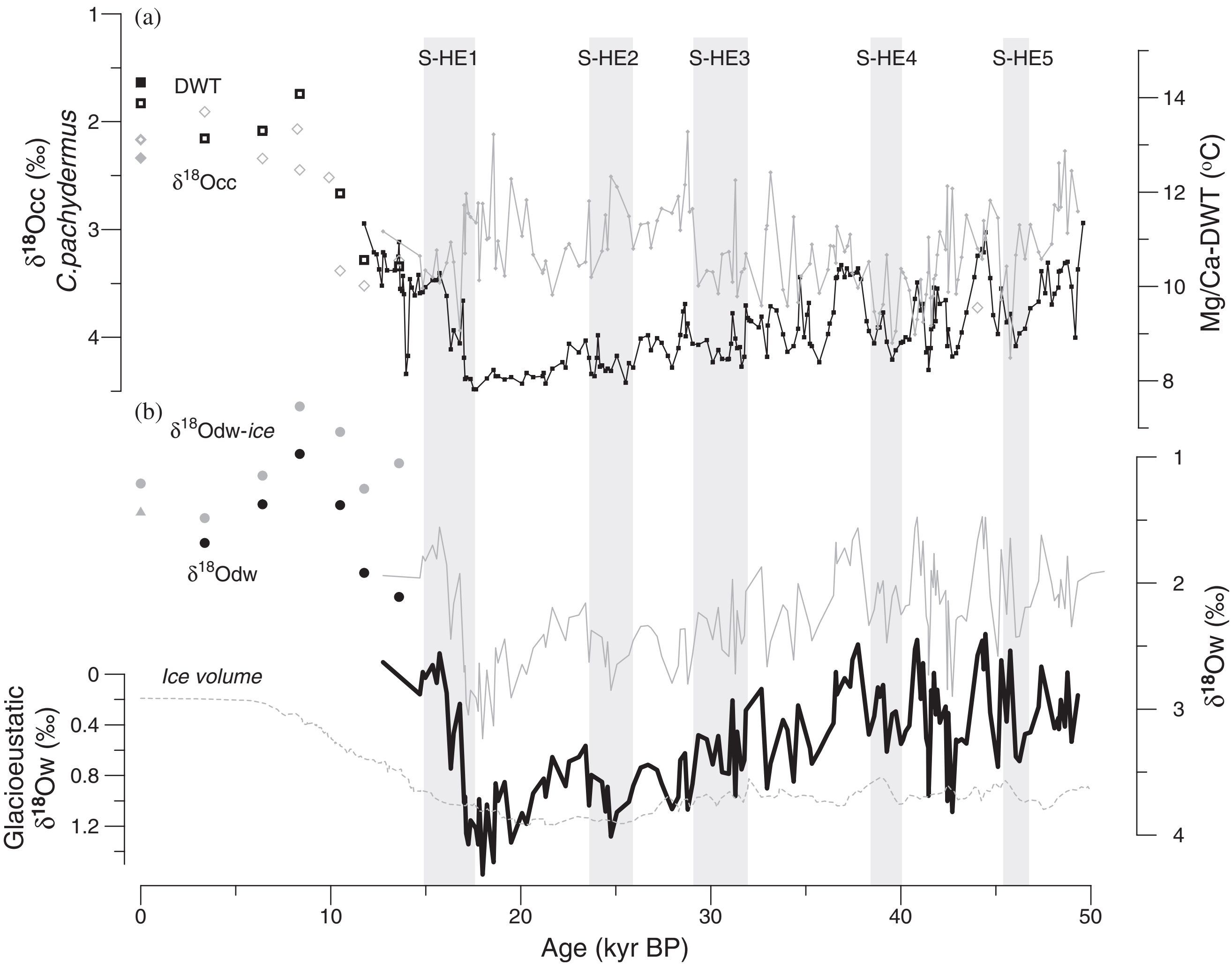

Fig. 5. (a) δ^{18}Occ in the benthic foraminifera *C. pachydermus* (continuous black line) and *Gyroidina* spp. (open black squares) compared to Mg/Ca estimates of Deep Water Temperature (DWT) based on *C. pachydermus* (continuous grey line) and *Gyroidina* spp. (open grey diamonds) from core MD95-2043. Average values of δ^{18}Occ (black filled square) and Mg/Ca DWT (black filled diamonds) of *C. pachydermus* and *Gyroidina* spp. Samples from core tops are also represented (core top points). (b) δ^{18}Odw estimate in core MD95-2043 after removing the DWT effect from the δ^{18}Occ measured in *C. pachydermus* (continuous black line) and *Gyroidina* spp. (black dots) and δ^{18}Odw after correction of the global effect of the ice sheets (δ^{18}Odw-ice) for those data measured in *C. pachydermus* (MD95-2043; continuous black line), *Gyroidina* spp. (grey dots) and *C. pachydermus* core tops (grey triangle). Vertical bars indicate the D–O stadials during which a Heinrich Event occurred in the North Atlantic Ocean (S-HE).

agreement with the core top estimates (see Section 3.2.2; Table 3). Glacial δ^{18}Odw shows a very clear D–O variability with relatively large oscillations (~0.5–1.2‰), showing higher/saltier and lower/fresher values during the stadials and interstadials, respectively, but this pattern is reversed for the S-HE3 and S-HE1, which show relatively, light δ^{18}Odw. δ^{18}Odw-ice values for the full glacial interval range between 3‰ and 1.7‰ (average 2.3‰), which are significantly higher than those of the present day WMDW (1.5‰). Current δ^{18}Odw values were only achieved during very brief intervals of the last MIS 3, in particular during the D–O interstadials 12, 10 and 8. In contrast, Early Holocene samples show anomalously light values in comparison to present δ^{18}Ow, but these Holocene measurements have been performed in *Gyroidina* spp. samples. Core top isotopic measurements of *Gyroidina* spp. show a rather large variability and the average value for the δ^{18}Odw estimates is about 0.2‰ lighter than that obtained from the *C. pachydermus* measurements. For this reason part of the lightening of the early Holocene δ^{18}Odw could be an artefact of the change in the benthic species. Nevertheless, the lightening is of about 0.5‰, and for some samples even greater (0.8‰), and the presence of a late Holocene δ^{18}Odw enrichment observed in the *Gyroidina* spp. measurements (Fig. 5) leads to the interpretation that δ^{18}Odw were indeed anomalously light for a time period between 13.6 and 8.4 cal ka BP, or probably longer since our resolution for this part of the record is very coarse. During this time period an organic-rich layer was formed in the Alboran Sea (Cacho et al., 2002) and oxygen conditions in the benthic layer were at a minimum (Caralp, 1988).

The comparison between glacial and present Mediterranean δ^{18}Ow data (Fig. 7a) illustrates a very different mixing line for these two periods. We have performed an estimation of past deep-water salinities (DWS) using the δ^{18}Ow:salinity equation estimated from present day water measurements (Section 2.3). The resulting DWS estimates (Fig. 6b) show an extremely large variability indicating palaeosalinities up to 41.5 psu for some of the glacial intervals. Obviously, the error that we are introducing into this reconstruction is very large, considering that the glacial mixing line was the same as the one for present Mediterranean waters (Schmidt, 1999). Changes in salinity may have been overestimated by assuming a constant δ^{18}Ow:salinity slope between glacial and interglacial periods. Although accurate glacial DWS can not be reconstructed since no modern analogue is available, high glacial δ^{18}Ow should still be related to enhanced evaporation versus precipitation and thus linked to higher salinities. In this way, the S–T diagram for benthic reconstructions (Fig. 6) should be, from a qualitative point of view, a valid representation for changes in WMDW densities. The densest WMDW were formed mostly during MIS 2, including S-HE2 and the early part of S-HE1 and during most of the D–O stadials. Lightest waters dominated during the D–O Interstadials (i.e. 8, 9, 10 and 12) and during the latest part of S-HE1. Densities during S-HE3, 4 and 5 stayed at an intermediate level. The very few points available for the early Holocene show densities comparable to or even lighter than those of present day WMDW.

3.3.2. Climatic implications of the deep-water variability

The SST record mostly reflects conditions of the Atlantic inflow, in contrast WMDW is formed in the Mediterranean Sea and its properties are controlled by climatic conditions over the Mediterranean. In order to better identify the potential signature of Mediterranean climate conditions on

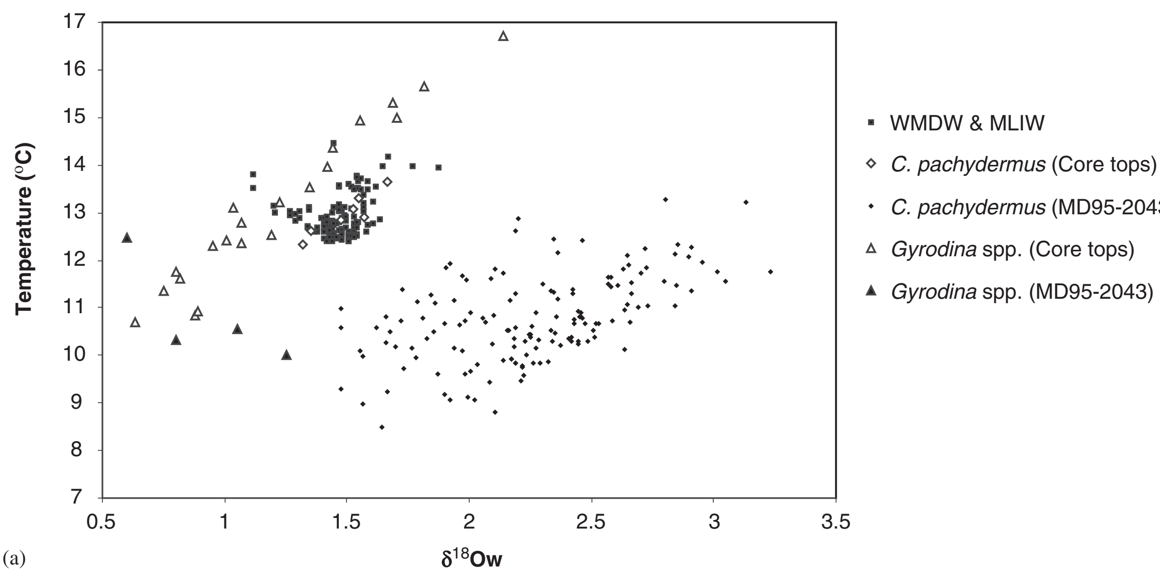

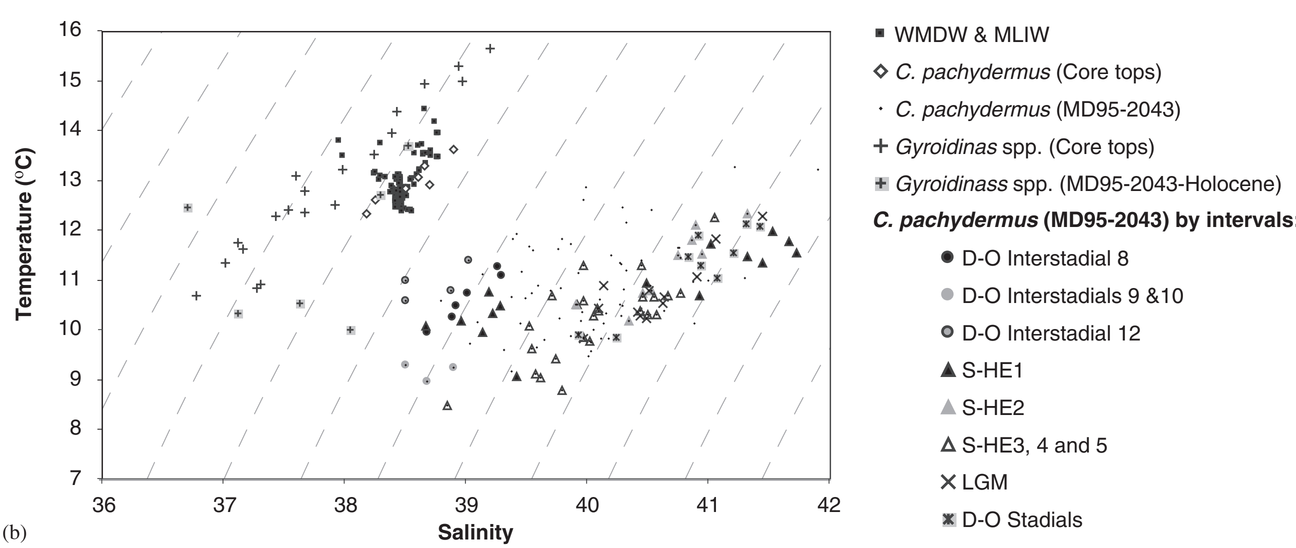

Fig. 6. (a) Temperature-δ^{18}Ow diagram and (b) temperature-salinity diagram for water samples (Pierre, 1999), *C. pachydermus* samples from core tops and *C. pachydermus* and *Gyroidina* spp. samples from core MD95-2043. See text for discussion on the palaeosalinity errors. Grey lines are isopicnas. WMDW-Western Mediterranean Deep Water; MLIW—Modified Levantine Intermediate Water.

the WMDW records these records are compared to pollen records from both sides of the Mediterranean Sea (Fig. 7): a pollen record from the same core MD95-2043, which mostly reflects vegetation changes in South Iberia (Sánchez Goñi et al., 2002) and a pollen record from the Ioannina basin, which reflects vegetation changes in Western Greece (Tzedakis et al., 2002; Tzedakis et al., 2004). The age model for the Ioannina record is independent to that of core MD95-2043 but in MIS 3 both records were correlated to the GISP2 core (Cacho et al., 1999; Tzedakis et al., 2004). At the Ioannina location, tree populations were far from their moisture tolerance threshold and in consequence the AP record can reflect the relative intensity of past climatic oscillations better than other regions closer to their tolerance limit (Tzedakis et al., 2004). Some of the most distinctive features in the DWT record are also present in Ioannina pollen (Fig. 7c) but they do not appear in either the SST record, or in the pollen record from MD95-2043 (Fig. 7b). As a result of this, S-HE4 stands out in both records as the most severe of the D–O stadials including those associated to other HEs. An enhanced HE4 signal has already been described in ice rafted detritus in the Portuguese margin (Thouveny et al., 2000) or polar source waters in the Alboran Sea (Cacho et al., 1999), but some low latitude processes also show a significant enhancement in the HE4 signal, as is the case in the northern transport of Saharan dust (Moreno et al., 2002). Interestingly, the relatively cold DWTs that dominated the S-HEs were achieved prior to the onset of the stadial according to the SST record (i.e. S-HE3; Fig. 7). This observation is supported by the common chronology of both surface and deep-water records, and it suggests that persistent cold conditions developed in some parts of the Mediterranean region before ($\sim$2 ka) the occurrence of major changes in the North Atlantic meridional overturning. The end of the S-HE3 is highlighted by a rapid increase in both the DWT and Ioannina records, indicating a rapid water warming while temperature and/or humidity conditions increased in Greece. Relatively high DWT values continued until the MIS 3/2 transition (24 ka BP), resulting in one of the warmest intervals of the glacial record. All these observations indicate that although Mediterranean millennial variability was governed by the North Atlantic D–O type of climatic variability, the intensity and in some cases the persistence, of these climatic oscillations were further modified by other regional processes (Fig. 7c). This interpretation is further supported by the record of *Emiliania huxleyi* $>$4 mm, a proxy for SST measured in the Menorca core MD99-2343 (Colmenero-Hidalgo et al., 2004). Surface waters at this location have been modified by Mediterranean conditions during its path from the Alboran Sea. This record shows a strong D–O signal, similar to that from the Alboran Sea SST record but it shares some peculiarities with the Alboran DWT record. In particular, the relatively cold values before, during and after S-HE4 and a relatively warm MIS 2 are common features between both surface and deep-water records, supporting the control of Mediterranean climate on these thermal changes. In contrast, the intensity and duration of the changes in Alboran SST and vegetation over S Iberia (Fig. 7b) seem to be modulated solely by D–O cycles in the N-Atlantic overturning circulation. Covariance between DWT and Ioannina pollen records disappears during MIS 2, the different climatic conditions of MIS 2 could have changed the limiting factor for vegetation evolution in the Ioannina basin.

Interestingly, neither δ^{18}Odw, nor δ^{13}C records show any of the specific features/structures described in the DWT and Ioannina pollen record. In any case all records agree in showing a D–O pacemaker in their millennial variability, but very remarkable differences emerge between the isotopic and DWT records. This situation suggests a sort of decoupling between the temperature and δ^{18}Odw signal from the WMDW. In a general sense, cold and heavy waters coexisted but the intensity of the changes evolved very differently. The coldest interval (S-HE4) does not stand out as the heaviest δ^{18}Odw values during the MIS 3 record and, in contrast, the heaviest WMDW occurred during MIS 2 but coexisted with relatively warm temperatures. δ^{18}Odw values should ultimately reflect changes in the evaporation–precipitation balance of the Mediterranean Sea, but the original δ^{18}Ow signal of the inflowing water could also exert an important influence on this record. A fresher Atlantic inflow could account for the presence of relatively light WMDW during HEs which would not have been expected for these intervals of enhanced evaporation due to the prevailing arid conditions (Combourieu-Nebout et al., 2002; Sánchez Goñi et al., 2002). Changes in the intensity and δ^{18}Ow composition of local runoff, for instance of the Rhone discharge in the Gulf of Lions, would also have an important effect in the δ^{18}Odw from WMDW (Rohling, 1999). In any case, the isotopic variability in both the Atlantic inflow and in the Gulf of Lions runoff is expected to be primarily controlled by the North Atlantic climatic variability (Combourieu-Nebout et al., 2002; Sánchez Goñi et al., 2002; Sierro et al., 2005) and these circumstances could ultimately account for the different patterns detected in the isotopic and DWT records. Additionally, Mediterranean δ^{18}Ow and salinity would also have been affected by changes in the residence time of the water masses in the Mediterranean Sea; longer residence time would have enhanced both δ^{18}Ow and salinity. Time residence is determined by the rate of water exchange through the Strait of Gibraltar controlled by global sea level changes. This effect could have been critical for the MIS 2 when the sea level was at its minimum, with the consequent reduction in the water exchange through Gibraltar. Model estimates indicate that even when Mediterranean excess evaporation remained constant at present values during the LGM, the MOW volume would have reduced substantially due to the low sea level and consequently, enhancing Mediterranean salinity (Rohling and Bryden, 1994). Changes in residence time of the Mediterranean waters

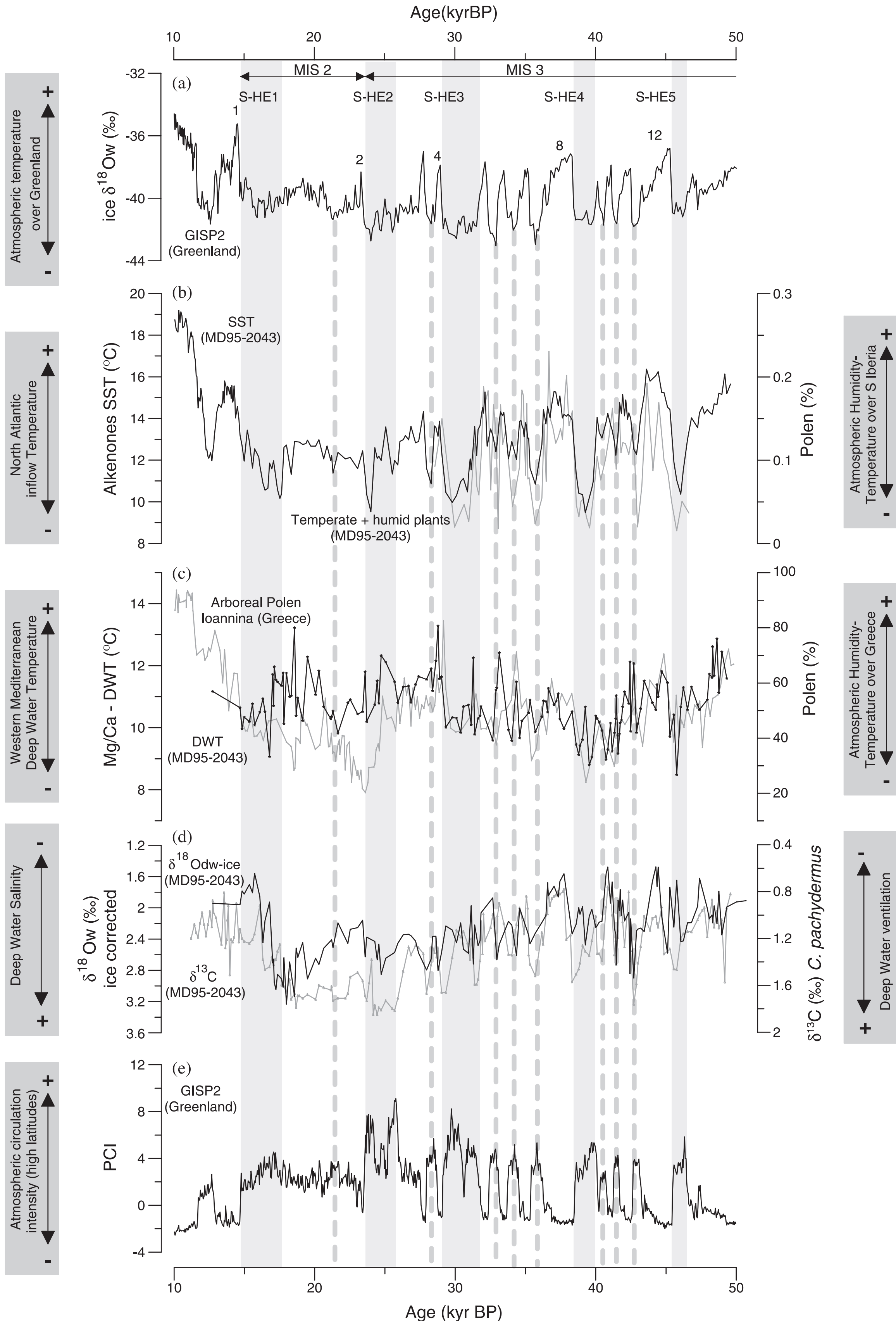

Age(kyrBP)
MIS 2
MIS 3
S-HE1
S-HE2
S-HE3
S-HE4
S-HE5
(a)
ice δ18Ow (‰)
GISP2 (Greenland)
Atmospheric temperature over Greenland
(b)
SST (MD95-2043)
Alkenones SST (°C)
Temperate + humid plants (MD95-2043)
Polen (%)
North Atlantic inflow Temperature
Atmospheric Humidity-Temperature over S Iberia
(c)
Arboreal Polen Ioannina (Greece)
DWT (MD95-2043)
Mg/Ca - DWT (°C)
Polen (%)
Western Mediterranean Deep Water Temperature
Atmospheric Humidity-Temperature over Greece
(d)
δ18Odw-ice (MD95-2043)
δ13C (MD95-2043)
δ18Ow (‰) ice corrected
δ13C (‰) C. pachydermus
Deep Water Salinity
Deep Water ventilation
(e)
GISP2 (Greenland)
PCI
Atmospheric circulation intensity (high latitudes)
Age (kyr BP)

would not affect DWT, which should primarily reflect climate conditions in the Mediterranean basin.

WMDW density is determined by DWT and DWS, which control deep-water convection in the Western Mediterranean and to some extent MOW into the Atlantic Ocean. Changes in WMDW ventilation are best represented by the δ^{13}C benthic records (Fig. 7d) and most of the oscillations are consistent with the δ^{18}Odw record, indicating improved ventilation during times of saltier waters. In spite of the large error associated with the DWS reconstruction it can still be a good qualitative proxy to infer relative changes in WMDW density (Fig. 6). Lowest density in glacial WMDW occurred mostly during D–O Interstadials, particularly 8, 9, 10 and 12 consistent with enhanced precipitation and runoff conditions indicated by pollen, geochemical and sedimentological records of the Western Mediterranean Sea (Combourieu-Nebout et al., 2002; Moreno et al., 2004; Sánchez Goñi et al., 2002). Similar low densities dominated the last part of the S-HE1 presumably related to the deglacial sea level rise, which enhanced Atlantic inflow and hence freshening Mediterranean waters. Consequently, MOW should have acquired buoyancy during these periods, resulting in a reduced flux in the lower/dense core of the MOW in the Gulf of Cadiz as supported by sedimentological and geochemical records from core MD99-2339 from the Gulf of Cadiz (Voelker et al., 2006). In contrast, maximum densities were recorded for most of the MIS 2, which is consistent with a strong and dense MOW flowing at deeper depths than today (Rogerson et al., 2005; Voelker et al., 2006). WMDW densities during the D–O stadials which were not associated to HEs recorded similar densities to MIS 2 which have also been correlated with events of intense and dense MOW in the contouritic record from the Gulf of Cadiz (Voelker et al., 2006). S-HE3, 4 and 5 present relatively high WMDW densities but not as high as the other stadials in agreement with the reduced ventilation, which occurred during part of these events (Sierro et al., 2005).

4. Conclusions

Paired isotopic and trace element measurements on different benthic species from a core top collection from the Western Mediterranean Sea suggest that this is a valid approach for the reconstruction of realistic WMDW conditions. These results also indicate the need to review the benthic Mg/Ca calibration for different regions and suggest that a correction of the global *Cibicidoides* calibration is needed for its application to the Western Mediterranean Sea, but this does not seem to be the case for other species such as *Uvigerinas* and *Gyroidina* spp.

The DWT record for the last glacial period shows relatively large oscillations (1–4 °C) in relation to the D–O cycles, with cold temperatures associated with stadial intervals. Nevertheless, this record shows features not immediately predicted by the "standard" D–O pattern and resemble vegetation changes described from Western Greece. S-HE4 was the coldest interval in the record and MIS 2 was a relatively warm interval. Both DWT and the pollen record from Greece suggest that a cold climate was installed in the Mediterranean before (~2 ka) major changes occurred in the North Atlantic overturning system in association to HE3, 4 and 5. S-HE3 ended with a striking rapid increase in both DWT and Ioannina records suggesting the occurrence of a major climatic change in the Mediterranean region towards warmer and probably wetter conditions. The different patterns between the DWT and SST record indicate a decoupling between the Mediterranean and the Atlantic climates at certain points, which needs further investigation.

δ^{18}Odw estimated by correction for Mg/Ca-DWT values exhibits large oscillations following a D–O pattern of variability, which mimics changes in WMDW ventilation rates as revealed by the benthic δ^{13}C records. δ^{18}Odw variability is interpreted as a result of the combination of three main factors: changes in the δ^{18}Ow composition of the Atlantic inflow and of the local runoff and in the residence time of the Mediterranean waters governed mostly by global sea level changes. These different factors accounted for the decoupling of the DWT and δ^{18}Odw records, which induced the persistence of a more pure D–O pattern of variability in the δ^{18}Odw records. Palaeosalinity reconstruction provides unrealistically high values suggesting the occurrence of changes in the water mixing line of the Mediterranean water masses during the glacial periods. DWT and DWS reconstructions are applied to obtain a semi-quantitative reconstruction of past changes in WMDW densities. Minimum glacial densities occurred mostly during D–O Interstadials and maximum during MIS 2 and D–O Stadial not associated to HEs. These changes in WMDW densities regulated the intensity and depth of the MOW in the Gulf of Cadiz.

Acknowledgements

We thank the specialist assistance of Mike Hall and Mervin Greaves; discussions and support with the ICP-OES measurements from Stephanie de Villiers; helpful

Fig. 7. (a) Ice δ^{18}O measured in GISP2 (Meese et al., 1997) (b) Alkenone Sea Surface Temperature (Cacho et al., 1999) and pollen percentages of humid and temperate plants (Sánchez Goñi et al., 2002) measured in core MD95-2043. (c) Estimated Deep Water Temperatures (DWT) based on *C. pachydermus* Mg/Ca ratios measured in core MD95-2043 and pollen percentages of Arboral Pollen (AP) measured in core Ioannina 284 from Western Greece (Tzedakis et al., 2004). (d) δ^{18}Odw-ice reconstruction compared to the δ^{13}C record from *C. pachydermus* (reversal *y*-axis). (e) Polar Circulation Index estimated from salt and dust content from Greenland ice core GISP2 (Mayewski et al., 1994).Vertical bars indicate the D–O stadials during which Heinrich Events occurred in the North Atlantic Ocean (S-HE).

reviews and comments on the manuscript by Luke Skinner, Stephen Barker and Chronis Tzedakis; and assistance with S–T plots from L. Pena. This research has been funded by the "POP project" (EC Grant: EVK2-2000-00089) and NERC Grant GR3/12889. IC thanks the support from the Comer foundation for abrupt climatic change research (USA) and from a Ramón y Cajal contract from the Spanish Ministry of Education and Science.

References

Anand, P., Elderfield, H., Conte, M.H., 2003. Calibration of Mg/Ca thermometry in planktonic foraminifera from a sediment trap time series. Palaeoceanography 18.

Barker, S., Greaves, M., Elderfield, H., 2003. A study of cleaning procedures used for foraminiferal Mg/Ca palaeothermometry. Geochemistry, Geophysics, Geosystems 4.

Barker, S., Cacho, I., Benway, H., Tachikawa, K., 2005. Planktonic foraminiferal Mg/Ca as a proxy for past oceanic temperatures: a methodological overview and data compilation for the Last Glacial Maximum. Quaternary Science Reviews 24, 1623–1636.

Béthoux, J.P., 1979. Budgets of the Mediterranean Sea. Their dependence on the local climate and on the characteristics of the Atlantic waters. Oceanologica Acta 2, 157–163.

Bigg, G.R., Wadley, M.R., 2001. Millennial-scale variability in the oceans: an ocean modelling view. Journal of Quaternary Science 16, 309–319.

Bigg, G.R., Jickells, T.D., Liss, P.S., Osborn, T.J., 2003. The role of the oceans in climate. International Journal of Climatology 23, 1127–1159.

Boyle, E.A., 1981. Cadmium, zinc, copper and barium in foraminifera test. Earth and Planetary Science Letters 53, 11–35.

Boyle, E.A., Keigwin, L.D., 1985. Comparison of Atlantic and Pacific palaeochemical records for the last 215.000 years: changes in deep ocean circulation and chemical inventories. Earth and Planetary Science Letters 76, 135–150.

Brown, F.H., Ederfield, H., 1996. Variations in Mg/Ca and Sr/Ca ratios of planktonic foraminifera caused by postdepositional dissolution: evidence of shallow Mg-dependent dissolution. Palaeoceanography 11, 543–551.

Cacho, I., Grimalt, J.O., Pelejero, C., Canals, M., Sierro, F.J., Flores, J.A., Shackleton, N.J., 1999. Dansgaard–Oeschger and Heinrich event imprints in the Alboran Sea palaeotemperatures. Palaeoceanography 14, 698–705.

Cacho, I., Grimalt, J.O., Sierro, F.J., Shackleton, N.J., Canals, M., 2000. Evidence of enhanced Mediterranean thermohaline circulation during rapid climatic coolings. Earth and Planetary Science Letters 183, 417–429.

Cacho, I., Grimalt, J.O., Canals, M., 2002. Response of the western Mediterranean Sea to the rapid climatic variability that occurred during the last 50,000 years: a molecular biomarker approach. Journal of Marine Systems 33–34, 253–272.

Caralp, M.H., 1988. Lateglacial to recent deep-sea benthic foraminifera from the Northeastern Atlantic (Cadiz Gulf) and Western Mediterranean (Alboran Sea): Palaeoceanographic results. Marine Micropaleontology 13, 265–289.

Colmenero-Hidalgo, E., Flores, J.-A., Sierro, F.J., Bárcena, M.Á., Löwemark, L., Schönfeld, J., Grimalt, J.O., 2004. Ocean surface water response to short-term climate changes revealed by coccolithophores from the Gulf of Cadiz (NE Atlantic) and Alboran Sea (W Mediterranean). Palaeogeography, Palaeoclimatology, Palaeoecology 205, 317–336.

Combourieu-Nebout, N., Turon, J., Zahn, R., Capotondi, L., Londeix, L., Pahnke, K., 2002. Enhanced aridity and atmospheric high-pressure stability over the western Mediterranean during the North Atlantic cold events of the past 50 ka. Geology 30, 863–866.

de Villiers, S., Greaves, M., Elderfield, H., 2002. An intensity ratio calibration method for the accurate determination of Mg/Ca and Sr/Ca of marine carbonates by ICP-AES. Geochemistry, Geophysics, Geosystems 3 (Paper number 2001GC000169).

Elderfield, H., Yu, J., Anand, P., Kiefer, T., Nyland, B., 2006. Calibrations for benthic foraminiferal Mg/Ca palaeothermometry and the carbonate ion hypothesis. Earth and Planetary Science Letters 250 (3–4), 633–649.

Ferguson, J.E., Henderson, G.M., Kucera, M., Rickaby, R.E.M., 2005. Trace element incorporation into planktonic foraminifera across a strong salinity gradient in the Mediterranean Sea. In: Biogeochemical Controls on Palaeoceanographic Proxies. The Geological Society, London.

Hodell, D.A., Charles, C.D., . Sierro, F.J., 2001. Late Pleistocene evolution of the ocean's carbonate system. Earth and Planetary Science Letters 192, 109–124.

Lacombe, H., Tchernia, P., Gamberoni, L., 1985. Variable bottom water in the Western Mediterranean Basin. Progress in Oceanography 14, 319–338.

Lambeck, K., Chappell, J., 2001. Sea-level change through the Last Glacial cycle. Science 292, 679–686.

Lea, D.W., Mashiotta, T.A., Spero, H.J., 1999. Controls on magnesium and strontium uptake in planktonic foraminifera determined by live culturing. Geochimica et Cosmochimica Acta 63 (16), 2369–2379.

Lea, D.W., Pak, D.K., Paradis, G., 2005. Influence of volcanic shards on foraminiferal Mg/Ca in a core from the Galápagos region. Geochemistry, Geophysics, Geosystems 6 (Q11P04).

Lear, C.H., Rosenthal, Y., 2005. Is temperature the sole environmental factor controlling benthic foraminiferal Mg/Ca? In: Biogeochemical Controls on Palaeoceanographic Proxies. The Geological Society, London.

Lear, C.H., Rosenthal, Y., Slowey, N., 2002. Benthic foraminiferal Mg/Ca-palaeothermometry: a revised core-top calibration. Geochimica et Cosmochimica Acta 66, 3375–3387.

Lewis, E., Wallace, D.W.R., 1998. Program developed for CO_2 system calculations, ORNL/CDIAC-105, Carbon Dioxide Information Analysis Center, Oak Ridge. National Laboratory, US Department of Energy, Oak Ridge, Tennessee.

Marchitto, T.M., deMenocal, P.B., 2003. Late Holocene variability of upper North Atlantic Deep Water temperature and salinity. Geochemistry, Geophysics, Geosystems 4.

Marchitto, T.M., Bryan, S.P., Curry, W.B., McCorkle, D.C. Linear Mg/Ca temperature calibration for the benthic foraminifer Cibicidoides pachyderma. Palaeoceanography, in press.

Martin, P.A., Lea, D.W., Rosenthal, Y., Shackleton, N.J., Sarnthein, M., Papenfuss, T., 2002. Quaternary deep sea temperature histories derived from benthic foraminiferal Mg/Ca. Earth and Planetary Science Letters 198, 193–209.

Mayewski, P.A., Meeker, L.D., Whitlow, S., Twickler, M.S., Morrison, M.C., Bloomfield, P., Bond, G.C., Alley, R.B., Gow, A.J., Grootes, P.M., Meese, D.A., Ram, M., Taylor, K.C., Wumkes, W., 1994. Changes in atmospheric circulation and ocean ice cover over the North Atlantic during the last 41,000 years. Science 263, 1747–1751.

MEDATLAS, 2002. Mediterranean and Black Sea database of temperature, salinity and Bio-chemical parameters climatological atlas. European Commission Marine Science and Technology Programme (MAST) Ed. 4 CD.

Meese, D.A., Gow, A.J., Alley, R.B., Zielinski, G.A., Grootes, P.M., 1997. The Greenland Ice Sheet Project 2 depth-age scale: Methods and results. Journal of Geophysical Research 102, 26411–26423.

Millot, C., 1990. The Gulf of Lions hydrodynamics. Continental Shelf Research 10, 885–894.

Mix, A.C., Bard, E., Schneider, R., 2001. Environmental processes of the ice age: land, oceans, glaciers (EPILOG). Quaternary Science Reviews 20, 627–657.

Moreno, A., Cacho, I., Canals, M., Prins, M.A., Sánchez Goñi, M.F., Grimalt, J.O., Weltje, G.J., 2002. Saharan dust transport and high-latitude glacial climatic variability: the Alboran Sea record. Quaternary Research 58, 318–328.

Moreno, A., Cacho, I., Canals, M., Grimalt, J.O., Sánchez-Vidal, A., 2004. Millennial-scale variability in the productivity signal from the Alboran Sea record, Western Mediterranean Sea. Palaeogeography, Palaeoclimatology, Palaeoecology 211, 205–219.

Moreno, A., Cacho, I., Canals, M., Grimalt, J., Sánchez Goñi, M.F., Shackleton, N.J., Sierro, F.J., 2005. Links between marine and atmospheric processes oscillating at millennial time-scale. A multi-proxy study of the last 50,000 yr from the Alboran Sea (Western Mediterranean Sea). Quaternary Science Reviews 24, 1623–1636.

Nürnberg, D., Bijma, J., Hemleben, C., 1996. Assessing the reliability of magnesium in foraminiferal calcite as a proxy for water mass temperatures. Geochimica et Cosmochimica Acta 60 (5), 803–814.

O'Neil, J.R., Clayton, R.N., Mayeda, T.K., 1969. Oxygen isotope fractionation in divalent metal carbonates. Journal of Chemical Physics 51.

Pena, L., Calvo, E., Cacho, I., Eggins, S., Pelejero, C., 2005. Identification and removal of Mn–Mg-rich contaminant phases in foraminiferal tests: Implications for Mg/Ca past temperature reconstructions. Geochemistry, Geophysics, Geosystems 6, Q09P02.

Pérez-Folgado, M., Sierro, F.J., Flores, J.A., Cacho, I., Grimalt, J.O., Zahn, R., Shackleton, N., 2003. Western Mediterranean planktonic foraminifera events and millennial climatic variability during the last 70 kyr. Marine Micropalaeontology 28, 49–70.

Pierre, C., 1999. The oxygen and carbon isotope distribution in the Mediterranean water masses. Marine Geology 153, 41–55.

Pinardi, N., Masetti, E., 2000. Variability of the large scale general circulation of the Mediterranean Sea from observations and modelling: a review. Palaeogeography, Palaeoclimatology, Palaeoecology 158, 153–173.

Reid, J.L., 1979. On the contribution of the Mediterranean Sea outflow to the Norwegian-Greenland Sea. Deep-Sea Research 26A, 1199–1223.

Rogerson, M., Rohling, E.J., Weaver, P.P.E., Murray, J.W., 2005. Glacial to interglacial changes in the settling depth of the Mediterranean Outflow plume. Palaeoceanography 20, PA3007.

Rohling, E.J., 1994. Review and new aspects concerning the formation of eastern Mediterranean sapropels. Marine Geology 122, 1–28.

Rohling, E.J., 1999. Environmental control on Mediterranean salinity and $\delta^{18}O$. Palaeoceanography 14, 706–715.

Rohling, E.J., Bryden, H.L., 1994. Estimating past changes in the Eastern Mediterranean freshwater budget, using reconstructions of sea level and hydrography. Proceedings of the Koninklijke Nederlandse Akademie van Wetenschappen Series B–Physical Sciences 97 (2), 201–217.

Rosenthal, Y., Boyle, E.A., Slowey, N., 1997. Temperature control on the incorporation of magnesium, strontium, fluorite and cadmium into benthic foraminiferal shells from Little Bahama Bank: prospects for thermocline palaeoceanography. Geochimica et Cosmochimica Acta 61, 3633–3643.

Rosenthal, Y., Lear, C.H., Oppo, D.W., Linsley, B.K., 2006. Temperature and carbonate ion effects on Mg/Ca and Sr/Ca ratios in benthic foraminifera: Aragonitic species Hoeglundina elegans. Palaeoceanography 21, PA1007.

Sánchez Goñi, M.F., Cacho, I., Turon, J.L., Guiot, J., Sierro, F.J., Peypouquet, J.-P., Grimalt, J.O., Shackleton, N.J., 2002. Synchroneity between marine and terrestrial responses to millennial scale climatic variability during the last glacial period in the Mediterranean region. Climate Dynamics 19, 95–105.

Schmidt, G.A., 1999. Error analysis of palaeosalinity calculations. Palaeoceanography 14, 422–429.

Shackleton, N.J., 1974. Attainment of isotopic equilibrium between ocean water and the benthonic foraminifera genus Uvigerina: isotopic changes in the ocean during the last glacial. In: Labeyrie, J. (Ed.), Les Méthodes Quantitatives d'étude des Variations du Climat au Cours du Pléistocène. Colloques Internationaux du CNRS. CNRS Paris, Gif/Yvette, pp. 203–210.

Siddall, M., Rohling, E.J., Almogi-Labin, A., Hemleben, C., Meischner, D., Schmelzer, I., Smeed, D.A., 2003. Sea-level fluctuations during the last glacial cycle. Nature 423, 853–858.

Sierro, F.J., Hodell, D.A., Curtis, J.H., Flores, J.A., Reguera, I., Colmenero-Hidalgo, E., Bárcena, M.Á., Grimalt, J., Cacho, I., Frigola, J., Canals, M., 2005. Impact of iceberg melting on Mediterranean thermohaline circulation during Heinrich events. Palaeoceanography 20.

Skinner, L.C., Elderfield, H., 2005. Constraining ecological and biological bias in planktonic foraminiferal Mg/Ca and $\delta^{18}O_{cc}$: a multispecies approach to proxy calibration testing. Palaeoceanography 20, PA1015.

Thouveny, N., Moreno, E., Delanghe, D., Candon, L., Lancelot, Y., Shackleton, N.J., 2000. Rock-magnetic detection of distal ice rafted debris: clue for the identification of Heinrich layers on the Portuguese margin. Earth and Planetary Science Letters 180, 61–75.

Tzedakis, P.C., Lawson, L.T., Frogley, M.R., Hewitt, G.M., Preece, R.C., 2002. Buffered tree population changes in a quaternary refugium: evolutionary implications. Science 297, 2044–2047.

Tzedakis, P.C., Frogley, M.R., Lawson, I.T., Preece, R.C., Cacho, I., de Abreu, L., 2004. Ecological thresholds and patterns of millennial-scale climate variability: the response of vegetation in Greece during the last glacial. Geology 32, 109–112.

Voelker, A.H.L., Lebreiro, S.M., Schonfeld, J., Cacho, I., Erlenkeuser, H., Abrantes, F., 2006. Mediterranean outflow strengthening during northern hemisphere coolings: a salt source for the glacial Atlantic? Earth and Planetary Science Letters 245, 39.

Zahn, R., Sarnthein, M., Erlenkeuser, H., 1987. Benthic isotope evidence for changes of the Mediterranean outflow during the late Quaternary. Palaeoceanography 2, 543–559.